IRCLASS
Indian Register of Shipping

CELEBRATING 50 YEARS OF EXCELLENCE

GUIDELINES ON **ASSESSMENT OF HULL GIRDER STRESSES DUE TO TORSION IN SHIPS WITH LARGE DECK OPENINGS**

SEPTEMBER 2024

Guidelines

Assessment of Hull Girder Stresses due to Torsion in Ships with large deck openings

September 2024

Contents

Sections

1. Introduction

1.1 Definitions
1.2 General

2. Procedure for Computation of Stresses due to Torsion

2.1 General
2.2 Formulation for assessment of stresses due to torsion

3. Evaluation of Cross-Sectional Properties

3.1 General
3.2 Co-ordinate System
3.3 Sectorial Co-ordinates
3.4 Pole
3.5 Principal Sectorial Co-ordinates
3.6 Principal Sectorial Statical Moment
3.7 Centroidal Sectorial Products of Area
3.8 Warping Constant
3.9 St.Venant's Constant
3.10 Method for evaluation of Cross-Sectional Properties

4. Application of Torsion Loads and Evaluation of Stresses

4.1 General
4.2 2D/3D Beam Finite Element Method
4.3 3D Finite Element Method

References

Appendix 1 – Example of evaluation of Cross-Sectional Properties for a Bulk Carrier Midship Section

Appendix 2 – Example of Evaluation of response of Container Ship Hull Girder to Torsion Loads

Section 1

Introduction

1.1 General

1.1.1 Part 3, Chapter 6 of the IRS *Rules and Regulations for Construction and Classification of Steel Ships* (hereinafter referred to as the Main Rules) require the assessment of stresses due to bending moments and torsion. This document is intended to provide guidance on the evaluation of stresses due to torsion. These Guidelines are intended for ships with large deck openings in the strength deck. A ship is regarded as one with large deck openings in strength deck if any one of the following conditions applies:

$$\frac{\mathbf{b}}{\mathbf{B_0}} > \mathbf{0.7}$$

$$\frac{\boldsymbol{\ell_1}}{\boldsymbol{\ell_0}} > \mathbf{0.89}$$

$$\frac{\boldsymbol{b}}{\boldsymbol{B_0}} > \mathbf{0.6}\ \boldsymbol{and}\ \frac{\boldsymbol{\ell_1}}{\boldsymbol{\ell_0}} > \mathbf{0.7}$$

where:

b = Breadth of the hatch opening, in [m]. Where there are multiple openings in the same hull transverse section, they are considered as a single opening, and b is calculated as the sum of the individual opening breadths. Refer Fig. 1.1.1

B_0 = Extreme breadth of deck measured, in [m] at the mid length of hatch opening. Refer Fig. 1.1.1

l_1= Length of the hatch opening, in [m]. Refer Fig. 1.1.1

l_0 = Distance, between centers of the deck strip at each end of the hatch opening, in [m]. Where there is no further hatch opening beyond the one under consideration, the point to which l0 is measured will be specially considered. Refer Fig. 1.1.1

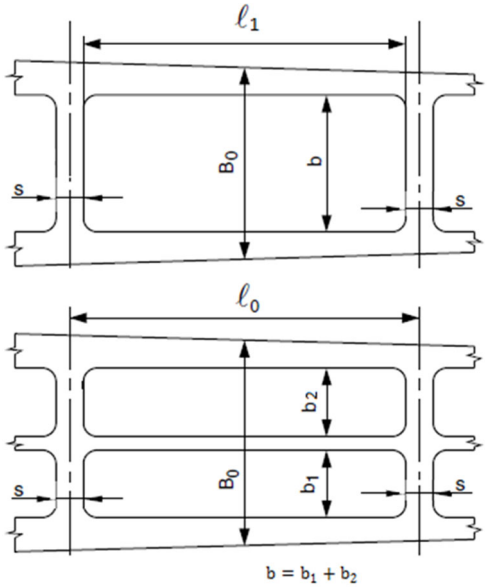

Fig.1.1.1: Ships with large deck openings

1.1.2 Torsion of the ship hull girder results in longitudinal and shear stresses on account of warping deformation (in addition to the shear stresses owing due to St. Venant torsion). These stresses are in the form of longitudinal axial stress and shear stress. The evaluation of these stresses is less straightforward as compared to the conventional hull girder bending stresses. It necessitates calculation of additional cross-sectional properties such as the *warping constant*, *torsion constant* and *statical*

moments of area. Likewise for evaluating the warping stress at a given location the "*sectorial coordinate*" is also required to be evaluated.

1.1.3 Consequently, the longitudinal axial stress and the shear stress due to warping from torsion loads should be accounted for when evaluating the longitudinal and the shear strength of the ship hull girder.

1.2 Definitions & Symbols

A_j	Directed area enclosed by the *j*th loop of the section, positive anticlockwise [m^2]
B	Bimoment [N-m^2]
C	Centroid of the ship section and origin of XYZ coordinate system [-]
E, G	Modulus of elasticity and shear modulus, respectively [N/m^2]
I_{yy}, I_{yz}, I_{zz}	Second moments of area of the section about the centroidal Y and Z axes [m^4]
$I_{y\omega}, I_{z\omega}$	Centroidal sectorial products of area [m^5]
$I_{\omega\omega}$	Warping constant [m^6]
J	Saint-Venant torsion constant [m^4]
L	Length of the ship between perpendiculars [m]
l_i	Length of the *i*th member within a ship section [m]
$m_T(x)$	Distributed total torsion (still water + wave) per unit length [Nm/m]
M_{ST}	Still Water Torsion Moment (kNm) (provided by the designer)
M_{WT}	Wave Torsion Moment (kNm) (Refer Part 3, Chapter 5, Section 3, Cl.3.7.5)
N	Number of independent loops in the ship hull girder section [-]
O	Origin of X_o, Y_o, Z_o (global) coordinate system [-]
r	Position vector of a node in the section with respect global origin '*O* '[m]
$\boldsymbol{r_p}$	Position vector of chosen pole P with respect to the global origin '*O*' [m]
s	Distance traversed along the section from a given node to another node [m]
S	Shear center of the beam section and origin of X_s, Y_s, Z_s coordinate system [-]
$S_{\omega s}$	Principal sectorial statical moment distribution of the cross-section [m^4]
S_{SV}	Saint-Venant statical moment [m^2]
t_i	Thickness of the *i*th member within a ship section [m]
$t(s)$	Thickness of the beam section members as a function of *s* [m]
T_{SV}	Saint-Venant torsion [N-m]
T_ω	Warping torsion [N-m]
y_{co}, z_{co}	Coordinates of the centroid C in the X_o, Y_o, Z_o coordinate system [m]
x	Longitudinal Co-ordinate measured across the length of the ship
y_{so}, z_{so}	Coordinates of the shear center S in the X_o, Y_o, Z_o coordinate system [m]
ω_{nc}	Normalized sectorial coordinate about Centroid [m^2]
ω_{nsc}	Normalized sectorial coordinate about Shear Center [m^2]
ω_p	Non-normalized sectorial coordinate about pole 'P' [m^2]
ω_{np}	Normalized sectorial coordinate about pole 'P' [m^2]
$\boldsymbol{\phi}$	Total angle of twist at a given cross section [rad]

Section 2

Procedure for Computation of Stresses due to Torsion

2.1 General

2.1.1 Evaluation of response to torsion loads may be performed using 2D/3D elastic beam theory or 3D finite element analysis of the full ship. The present guideline discusses the evaluation of response using the 2D elastic beam theory. For analyses using full ship 3D finite element models, refer to the IRS Guidelines on Structural Assessment of Ships based on Finite Element Method.

2.1.2 The objective of the approach using the 2D/3D elastic beam theory is to simplify the evaluation of the torsion response of the ship hull girder as a whole so that the axial stresses and the shear stresses due to the torsion are accounted for during assessment of longitudinal and shear strength of the hull girder. However, where detailed stresses are required to be computed for assessment of local structures, the 3D finite element analysis approach should be selected.

2.1.3 The following steps are followed to evaluate the stresses arising out of torsion moments.

1. Evaluation of Cross-Section properties
2. Application of Torsion loads on the Ship hull girder
3. Evaluation of Response to Applied Torsion Loads
4. Evaluation of Stresses

2.2 Formulation for assessment of stresses due to torsion

Analytical Technique

2.2.1 The assessment of the hull girder stresses due to torsion loads is performed by solving the differential equation as provided below:

$$\frac{\partial^2}{\partial x^2}\left(EI_{\omega\omega}\frac{\partial^2 \emptyset}{\partial x^2}\right) - \frac{\partial}{\partial x}\left(GJ\frac{\partial \emptyset}{\partial x}\right) = m_T(x) \quad x = \{0: L\} \qquad (2.1)$$

2.2.2 Appropriate boundary conditions are to be chosen so as to reflect the warping displacement and the angle of twist profile of the ship hull girder. As an example, for a container ship with a single island configuration (i.e. Engine Room and Deckhouse located at the same longitudinal position), the warping and angle of twist are selected to be zero since the hull girder cross section at the Engine Room has much superior torsional rigidity and resistance to warping (i.e., ϕ=0 and $d\phi/dx$=0 at x = X_{ER}). The total torsion (sum of T_{SV} and T_{ω}) and Bi-Moment at both ends of the ship are zero. This is applicable for solving the differential equation analytically.

2.2.3 The distributed torsion per unit length ($m_T(x)$) is determined from equation 2.2. The computation of $I_{\omega\omega}$ and J is described in Section 3.8 and 3.9 respectively. These quantities should be evaluated for several longitudinal positions (atleast 15) along the ship hull girder to represent the variation of hull girder torsional rigidity and warping constants along the length of the ship.

$$m_T(x) = 1000\frac{d(M_{ST} + M_{WT})}{dx} \qquad (2.2)$$

2.2.4 Upon solution of equation 2.1, the Bi-Moment, St. Venant and Warping Torsion can be evaluated as shown below:

$$B(x) = EI_{\omega\omega}\frac{\partial^2 \emptyset}{\partial x^2} \qquad (2.3)$$

$$T_{\omega}(x) = -\frac{\partial B}{\partial x} = -\frac{\partial}{\partial x}\left(EI_{\omega\omega}\frac{\partial^2 \emptyset}{\partial x^2}\right) \qquad (2.4)$$

$$T_{SV}(x) = GJ\frac{\partial \emptyset}{\partial x} \qquad (2.5)$$

2.2.5 The warping axial stress (longitudinal) and warping shear stresses are then evaluated as shown below:

$$\sigma_{xx}(x,s) = -\left(\frac{B(x)}{I_{\omega\omega}(x)}\right)\omega_{nsc}(x,s) \qquad (2.6)$$

$$\tau_{xs}(x,s) = -\left(\frac{T_{\omega}(x)}{t(s)I_{\omega\omega}(x)}\right)S_{\omega s}(x,s) - \left(\frac{T_{SV}(x)}{t(s)J(x)}\right)S_{SV}(x,s) \qquad (2.7)$$

Finite element method

2.2.6 Finite element analysis using 2D/3D beam elements may also be used to solve the Equation 2.1. When using commercially available computer programs with 2D/3D beam elements, verification of the accuracy of the computer program should be performed with test cases in the literature.

2.2.7 The Ship hull girder is idealized as an elastic beam subjected to torsion loads along its length. The beam is further discretized using several 2D/3D beam finite elements, each with two nodes. Each node possesses the warping and the angular rotation (angle of twist) degrees of freedom with regard to Torsion evaluation.

2.2.8 Each of the 2D/3D beam finite elements require evaluation of the torsional rigidity constant (J) and the warping constant ($I_{\omega\omega}$). These are less straight-forward to evaluate as compared to the moments of inertia and the cross-sectional area. Notably, these properties vary with the ship hull cross section. The evaluation of these cross-section properties is described in Section 3.

2.2.9 The stiffness matrix considering the angular rotation and the warping degrees of freedom for the beam elements may be considered based upon recognized elastic torsion theories for beams (please refer the pertinent literature listed in the References section).

2.2.10 Appropriate boundary conditions should be selected based upon the torsional rigidity and warping resistance of the ship hull girder. As an example, for a container ship with a single island configuration (i.e. Engine Room and Deckhouse located at the same longitudinal position), the warping and angle of twist are selected to be zero.

2.2.11 Notwithstanding the requirements in 2.2.6 to 2.2.10, a full ship 3D finite element model may also be used for evaluation of warping induced axial longitudinal stresses and shear stresses as well as torsion induced shear stresses. This may be especially useful for direct evaluation for loads corresponding to different static and dynamic load conditions (e.g. combination of various stresses from static and dynamic vertical and horizontal bending moments as well as horizontal and vertical shear forces). The development of the finite element model, application of loads and boundary conditions and combination of stresses for final assessment should be agreed with IRS prior to performing such analysis.

Section 3

Evaluation of Cross-Sectional Properties of the Hull Girder

3.1 General

3.1.1 This section describes in detail the evaluation methodology for the cross sectional properties of the hull girder relevant to evaluation of stresses due to torsion moments.

3.2 Co-ordinate system

3.2.1 The X_o axis is directed along the length of the ship, whereas the Y_o and Z_o axes lie in transverse plane. The Y_o axis is directed along the beam of the ship (i.e. transverse direction) and the Zo axis is directed along the depth (i.e. vertical). The origin of the section may be placed anywhere in the transverse plane. The coordinate systems XYZ and X_s, Y_s, Z_s are parallel to the X_o, Y_o, Z_o system and passing through the centroid and the center of twist (i.e., shear center) of the ship, respectively. The right-hand thumb rule is applicable and hence, areas and vector products are positive anticlockwise.

Figure 3.2.1 provides an illustration of the co-ordinate system.

3.3 Sectorial Co-ordinates

3.3.1 For evaluation of warping of cross section, a warping function needs to be defined. For thin- walled beams the warping function reduces to the sectorial coordinate. For thin-walled members, the sectorial coordinate is approximated as a single value along the thickness of the member at its centerline. It is named thus due to its equivalence with the conventional y-z coordinates in terms of its formulae. The sectorial coordinate is calculated about an arbitrarily chosen pole (defined in section 3.4). The sectorial coordinate about a pole 'P' is a vector product given by

$$\overrightarrow{\boldsymbol{\omega_p}}(s) = \int_0^s \left(\vec{\boldsymbol{r}}(s) - \overrightarrow{\boldsymbol{r_p}}(s)\right) \times \overrightarrow{\boldsymbol{ds}} \qquad (3.1)$$

3.3.2 The sectorial coordinate is in the axial ('X') direction. For convenience, only the magnitude is dealt with in the calculations related to the sectorial coordinate. Integration is started with an arbitrary point on the section chosen as the starting point. The sectorial coordinate is normalized by subtracting from its distribution, its mean value over the entire section, as given in (3.2).

$$\omega_{np}(s) = \omega_p(s) - \frac{1}{\int_A ds} \int_0^{\int_A ds} \omega_p \, ds \qquad (3.2)$$

3.4 Pole

3.4.1 A pole is an arbitrary reference point in the plane of the cross-section about which position vectors are measured for the calculation of sectorial coordinate.

3.5 Principal Sectorial Co-ordinates

3.5.1 The principal sectorial coordinate is the sectorial coordinate considering the shear center as pole.

3.6 Principal Sectorial Statical Moment

3.6.1 It is the first moment of area of the principal sectorial coordinate. The change in the sectorial statical moment between two points on the section is given by (3.3).

$$\Delta S_{\omega s} = \int_{s_1}^{s_2} \omega_{nsc} dA \qquad (3.3)$$

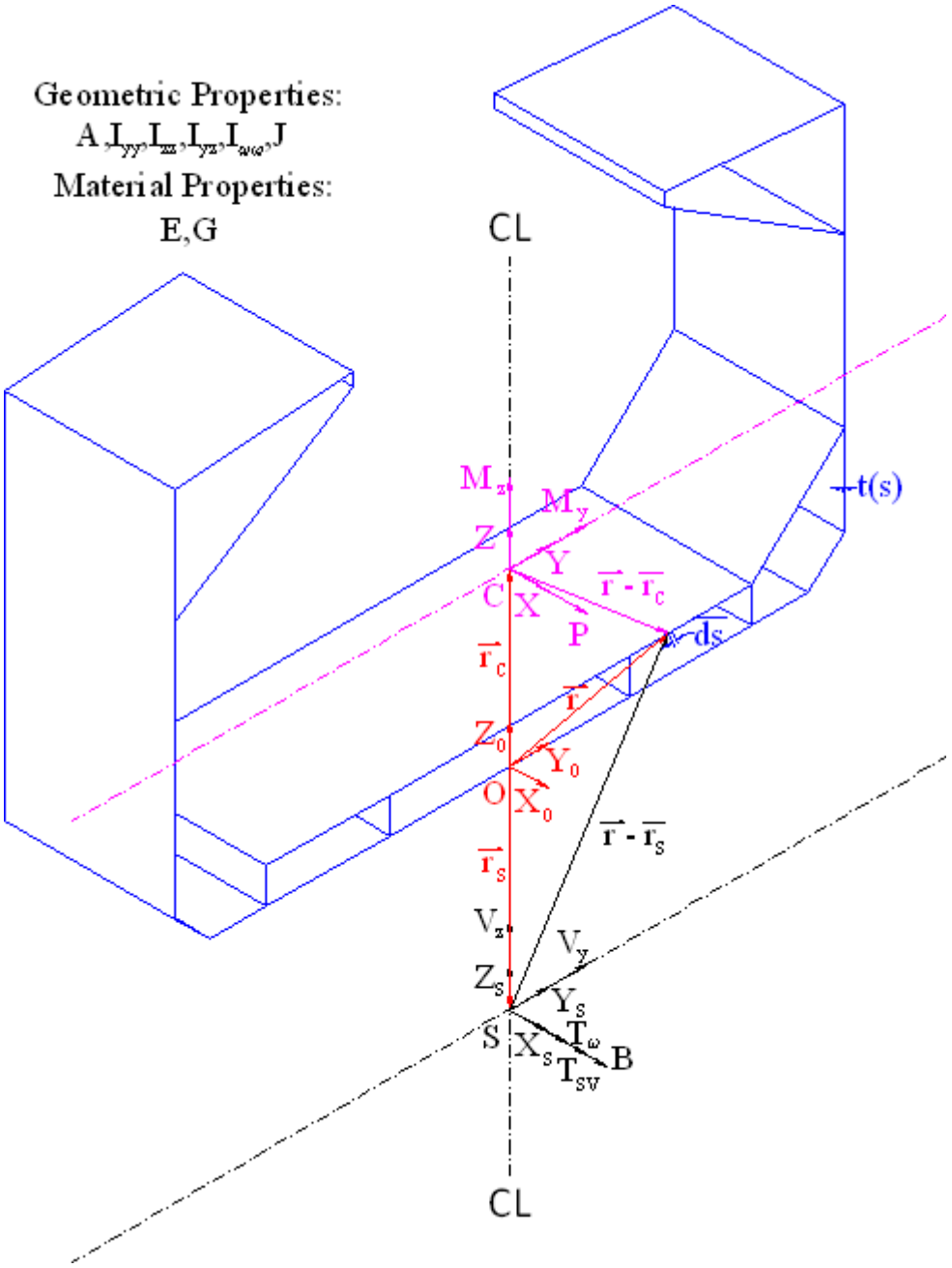

Figure 3.1.1 – Co-ordinate system for calculation of cross section properties and application of loads

3.7 Centroidal Sectorial Products of Area

3.7.1 The products of Iyω and Izω are defined with respect to the sectorial coordinate about the centroid as the pole and the 'Y' or 'Z' axis, respectively. Sectorial products of area are zero when the chosen pole is the shear center. They are given by (3.4)

$$I_{y\omega} = \int_{\Omega} (z_o - z_{c,o})\omega_{nc} dA$$
$$I_{z\omega} = \int_{\Omega} (y_o - y_{c,o})\omega_{nc} dA \qquad (3.4)$$

3.8 Warping Constant

3.8.1 It is the second moment of area of the principal sectorial coordinate and is given by (3.5).

$$I_{\omega\omega} = \int_{\Omega} \omega_{nsc}^2 \, dA \qquad (3.5)$$

3.9 St. Venant Torsion Constant

3.9.1 It is the rigidity of the section against Saint-Venant torsion, and is related to the enclosed area of independent loops in the section. The set of equations (3.6) to (3.8) are used for finding the torsion constant, where the applied Saint-Venant torsion T_{SV} is an arbitrary non-zero value, Aj's are the areas of the loops, χ_ij is used to account for the direction of integration of the loops and q_j^id's are the indeterminate Saint-Venant shear flows.

$$\begin{bmatrix} \oint_1 \frac{\chi_{11}(s)ds}{t(s)} & \oint_1 \frac{\chi_{12}(s)\,ds}{t(s)} & \cdots & \oint_1 \frac{\chi_{1N}(s)\,ds}{t(s)} & -2A_1 \\ \oint_2 \frac{\chi_{21}(s)\,ds}{t(s)} & \oint_2 \frac{\chi_{22}(s)ds}{t(s)} & \cdots & \oint_2 \frac{\chi_{2N}(s)\,ds}{t(s)} & -2A_2 \\ \vdots & \vdots & \ddots & \vdots & \vdots \\ \oint_N \frac{\chi_{N1}(s)\,ds}{t(s)} & \oint_N \frac{\chi_{N2}(s)\,ds}{t(s)} & \cdots & \oint_N \frac{\chi_{NN}(s)\,ds}{t(s)} & -2A_N \\ 2A_1 & 2A_2 & \cdots & 2A_N & \frac{1}{3}\sum_i l_i t_i^3 \end{bmatrix} \begin{pmatrix} q_1^{id} \\ q_2^{id} \\ \vdots \\ q_N^{id} \\ G\emptyset' \end{pmatrix} = \begin{pmatrix} 0 \\ 0 \\ \vdots \\ 0 \\ T_{SV} \end{pmatrix} \qquad (3.6)$$

$$\chi_{ij} = \begin{cases} -1 & for\ members\ common\ to\ loops\ i\ and\ j\ with\ opposite\ direction \\ 0 & for\ members\ not\ common\ between\ loops\ i\ and\ j \\ 1 & for\ members\ common\ to\ loops\ i\ and\ j\ with\ same\ direction \end{cases} \qquad (3.7)$$

$$J = \frac{T_{SV}}{G\emptyset'} \qquad (3.8)$$

3.10 St. Venant Statical Moment (S_{SV})

3.10.1 It is defined as the shear flow (in the absence of any other forces or moments on the section) per unit Saint-Venant torsion multiplied by its Saint-Venant torsion constant and is given by (3.9). Saint-

Venant statical moment is zero in parts of the section which do not belong to any loop and is piecewise constant between any two consecutive nodes of a member within a section.

$$S_{SV}(s) = -\frac{q(s)J}{T_{SV}} \qquad (3.9)$$

3.11 Method for evaluation of Cross Section Properties

3.11.1 The sectorial properties ω_{nsc}, $S_{\omega s}$, S_{SV}, $I_{\omega\omega}$ and *J* are required for the analysis of ships for torsion.

Following are the steps for finding the aforementioned properties for any given transverse section:

.1 Apply an arbitrary non-zero Saint-Venant torsion T_{SV} and find the Saint-Venant torsion constant *J* of the section by solving the set of equations (3.6) to (3.8). The number of equations is one more than the total number of independent loops in the section.

.2 Superimpose the shear flows q_j^{id} of the various loops to find the shear flow distribution *q(s)*.

.3 Find the distribution of S_{SV} using (3.9), q(s) and J. Note that S_{SV} is zero for parts of the section that are open, i.e., that do not belong to any loops and are piecewise constant in between any two consecutive nodes of a member in a given cross-section.

.4 If no loops exist, this step is skipped. If loops do exist, then create virtual slits in the section. The position of the slits must be chosen in a manner that ensures that no member of the section gets completely disconnected from the section, i.e., a single structure is maintained after the creation of slits.

.5 A set of paths is chosen for the calculation of sectorial coordinate. Choose a random point on the section as a starting point. At this stage, all paths are chosen such that each member is traversed exactly once, paths are always started at a previously visited node (except for the starting point) and the path continues (randomly) till a free end node (i.e., a node from which only a single member is passing through) is encountered. The entire structure is guaranteed to be covered in this manner.

.6 Calculate the temporary determinate non-normalized sectorial coordinate ω_c^d with the centroid as the pole using (3.1) and noting that the temporary value of the sectorial coordinate at each starting point is the same as its value in a previously visited path, the temporary value at the starting node being zero. The actual non-normalized sectorial coordinate about the centroid after compatibility conditions are applied is given by (3.10).

$$\omega_c(s) = \omega_c^d(s) + \int_0^s \frac{S_{SV}(s)}{t(s)} ds \qquad (3.10)$$

.7 Normalize the sectorial coordinate about the centroid to obtain ω_{nc} using (3.2).

.8 Find the sectorial products of area about the centroid using (3.4).

.9 Find the position of the shear center using (3.11).

$$y_{s,o} = y_{c,o} + \frac{I_{zz}I_{y\omega} - I_{yz}I_{z\omega}}{I_{yy}I_{zz} - I_{yz}^2}$$
$$z_{s,o} = z_{c,o} + \frac{I_{yz}I_{y\omega} - I_{yy}I_{z\omega}}{I_{yy}I_{zz} - I_{yz}^2} \quad (3.11)$$

.10 Repeat the steps 6 and 7 with the shear center as the pole instead of the centroid in order to obtain the principal sectorial coordinate ω_{nsc}.

.11 Calculate the warping constant $I_{\omega\omega}$ of the section using (3.5).

.12 The next step is to calculate the determinate part of first moment of area of the principal sectorial coordinate, i.e., $S_{\omega s}$. For that, a set of paths has to be chosen, the methodology of which is different from the set of paths used for the sectorial coordinate. At this stage, all paths are chosen such that each member is traversed exactly once, paths are always started at a node from which exactly one unvisited member exists and the path continues till a bridge node (i.e., a node from which at least three members are passing through after the creation of virtual slits, if any) is encountered. The entire structure is guaranteed to be covered in this manner. The same set of virtual slits in step 4, if any, may be used.

.13 Calculate the determinate part of $S_{\omega s}$ using (3.3). Note that the starting value of $S_{\omega s}$ in each path new path in a direction away from the starting node along that path is the sum of all the values of $S_{\omega s}$ flowing in the direction of that node from all previously visited paths ending at that node.

.14 If loops do not exist, then this step is skipped and $S_{\omega s}$ found in step 13 is the final value of $S_{\omega s}$. If loops do exist, then the compatibility condition (3.12) is applied to find the indeterminate part of $S_{\omega s}$. For consideration of direction of flow path, χ_{ij} from (3.7) is used. The number of equations in this case is same as the number of independent loops in the section.

$$\begin{bmatrix} \oint_1 \frac{\chi_{11}(s)ds}{t(s)} & \oint_1 \frac{\chi_{12}(s)\,ds}{t(s)} & \cdots & \oint_1 \frac{\chi_{1N}(s)ds}{t(s)} \\ \oint_2 \frac{\chi_{21}(s)\,ds}{t(s)} & \oint_2 \frac{\chi_{22}(s)ds}{t(s)} & \cdots & \oint_2 \frac{\chi_{2N}(s)\,ds}{t(s)} \\ \vdots & \vdots & \ddots & \vdots \\ \oint_N \frac{\chi_{N1}(s)\,ds}{t(s)} & \oint_N \frac{\chi_{N2}(s)\,ds}{t(s)} & \cdots & \oint_N \frac{\chi_{NN}(s)\,ds}{t(s)} \end{bmatrix} \begin{pmatrix} S^{id}_{\omega s,1} \\ S^{id}_{\omega s,2} \\ \vdots \\ S^{id}_{\omega s,N} \end{pmatrix} = - \begin{pmatrix} \oint_1 \frac{S^{d}_{\omega s,1}(s)}{t(s)} ds \\ \oint_2 \frac{S^{d}_{\omega s,2}(s)}{t(s)} ds \\ \vdots \\ \oint_N \frac{S^{d}_{\omega s,N}(s)}{t(s)} ds \end{pmatrix} \quad (3.12)$$

.15 The determinate and indeterminate parts of $S_{\omega s}$ are superimposed member-wise to obtain its final value. For superimposition, the indeterminate parts of all loops to which a member belongs are respectively either added to or subtracted from the determinate values in that member according to whether the direction of the integration of loop in (3.12) is same as the direction path of determinate $S_{\omega s}$ at that member.

3.11.2 A practical demonstration of the above steps is provided in Appendix 1.

Section 4

Application of Torsion Loads and Evaluation of Stresses

4.1 General

4.1.1 Application of Torsion Moment Loads should be in accordance with Part 3, Chapter 5, Section 3, 3.6.4 of the Main Rules. Direct calculations of these loads may be specially considered by IRS however these should not be less stringent than the loads evaluated using Part 3, Chapter 5, Section 3, 3.6.4 of the Main Rules.

4.1.2 Strength and Fatigue limit states should be separately considered. For Torsion moment loads evaluated using direct calculations, IRS may give special considerations provided that the designer contacts IRS early during the design process and furnishes all necessary information (which may also include the load calculation and stress assessment computational programs).

4.2 2D/3D Beam Finite Element Method

4.2.1 The distribution of the torsion loads should be applied on the beam model in accordance with Section 4.1. The equations 2.1 – 2.5 should be solved to obtain the following quantities at the given frame location(s) of evaluation:

1. Bimoment ($N.m^2$)
2. St. Venant Torsion (N.m)
3. Warping Torsion (N.m)

4.2.2 The evaluated distribution of the Bimoment, St. Venant Torsion and Warping Torsion should be presented in the report for each load case.

4.2.3 Using quantities obtained as described in 4.2.1, the stress evaluation should be performed as shown in equations 2.6 – 2.7.

Appendix 2 describes the process of evaluation of the hull girder stresses from torsion considering the example of a containership.

4.3 3D Finite Element Method

4.3.1 Torsion Loads should be applied using an appropriate method/technique so as to simulate the effect of Torsion moment distribution on the Ship.

4.3.2 With the use of full-ship 3D finite element, stresses are directly obtained after solving for the various load cases. The longitudinal and shear stresses should be extracted from the finite element model using appropriate techniques for further use for checking the longitudinal strength of the hull girder.

References

[1] IRS Rules for Construction and Classification of Bulk Carriers and Oil Tankers. July 2023.

[2] Alfano, G., Marotti de Sciarra, F., and Rosati, L. (1996). “Automatic analysis of multicell thin-walled sections,” *Computers & Structures*, vol. 59, no. 4, pp. 641-655.

[3] Edlund, S. (1997). “Arbitrary thin-walled cross sections. Theory and computer implementation,” *Licentiate thesis, Department of Structural Engineering, The Royal Institute of Technology, Stockholm, Sweden.*

[4] Pilkey, W.D. (2002). Analysis and design of elastic beams. First Ed. John Wiley & Sons, Inc. DOI: http://dx.doi.org/10.1002/9780470172667

[5] Slivker, V. (2007). Mechanics of structural elements: theory and applications. Springer.

[6] Schulz, M., and Filippou, F. (1998). “Generalized warping torsion formulation,” *Journal of Engineering Mechanics, American Society of Civil Engineers*, Vol. 124, pp 339 – 347.

[7] Waldron, P. (1986). “Sectorial properties of straight thin-walled beams,” *Computers and Structures*, Vol. 24, pp 147 – 156.

[8] *Project no. RRD13030-RR* (2014). “Development of procedure to evaluate stresses in hull girder section due to torsion loads,”*,*

[9] *Project no. RRD13018-RR* (2013). “Simplified procedure for analysis of shear stresses in ship hull girders using FE software

Appendix 1 - Illustration of detailed Section Properties calculations for Torsion for a bulk carrier section

For the purpose of illustration of cross sectional properties for torsion, a bulk carrier cross section is chosen. The same section is also used for illustration in IRS Rules for Bulk Carriers and Oil Tankers, Volume 2, Part 1, Chapter 5, Appendix 5. The geometry of the hull and its elements are listed in Tables A1.1 and A1.2 and shown in Fig. A1.1. The positions of virtual slits created and the paths that are chosen for the calculation of sectorial coordinate are shown in Fig. A1.2.

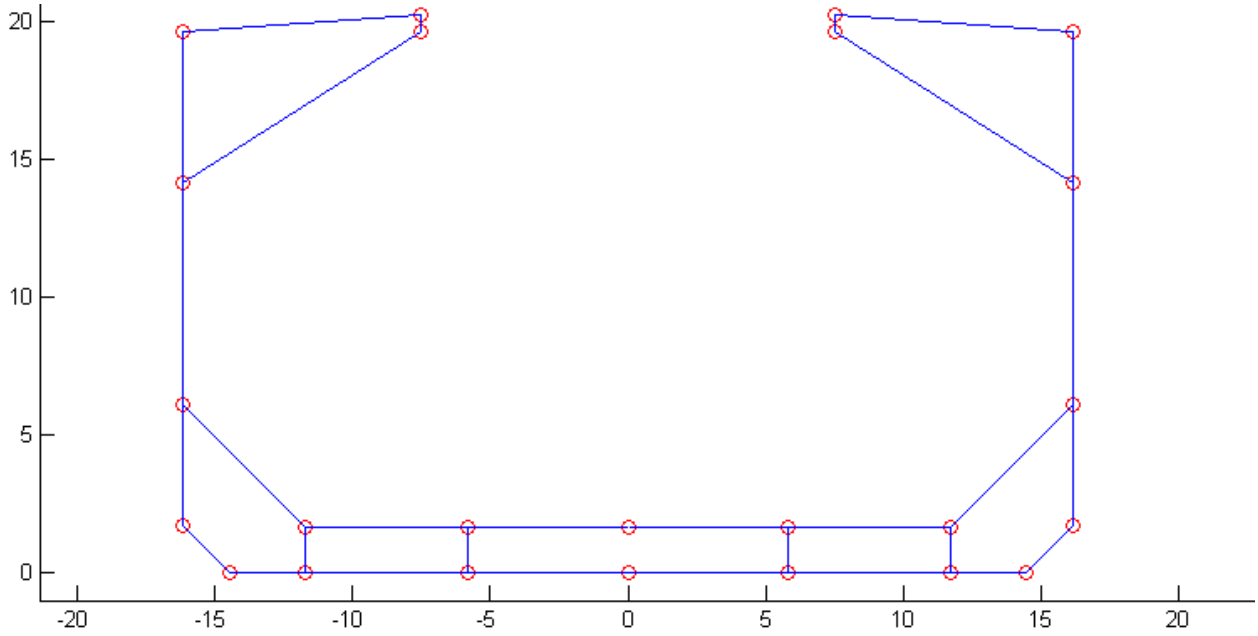

Fig. A1.1. Illustrative Ship hull girder section given in [3]. (Axes dimensions in 'm')

Table A1.1: Node coordinates of the idealized ship hull section

Node no.	Y Co-ordinate (m)	Z Co-ordinate (m)	Node no.	Y Co-ordinate (m)	Z Co-ordinate (m)
0	0.00	0.00	12	7.50	19.63
1	5.80	0.00	13	-5.80	0.00
2	11.70	0.00	14	-11.70	0.00
3	14.42	0.00	15	-14.42	0.00
4	16.13	1.72	16	-16.13	1.72
5	16.13	6.11	17	-16.13	6.11
6	11.70	1.68	18	-11.70	1.68
7	5.80	1.68	19	-5.80	1.68
8	0.00	1.68	20	-16.13	14.15
9	16.13	14.15	21	-16.13	19.60
10	16.13	19.60	22	-7.50	20.25
11	7.50	20.25	23	-7.50	19.63

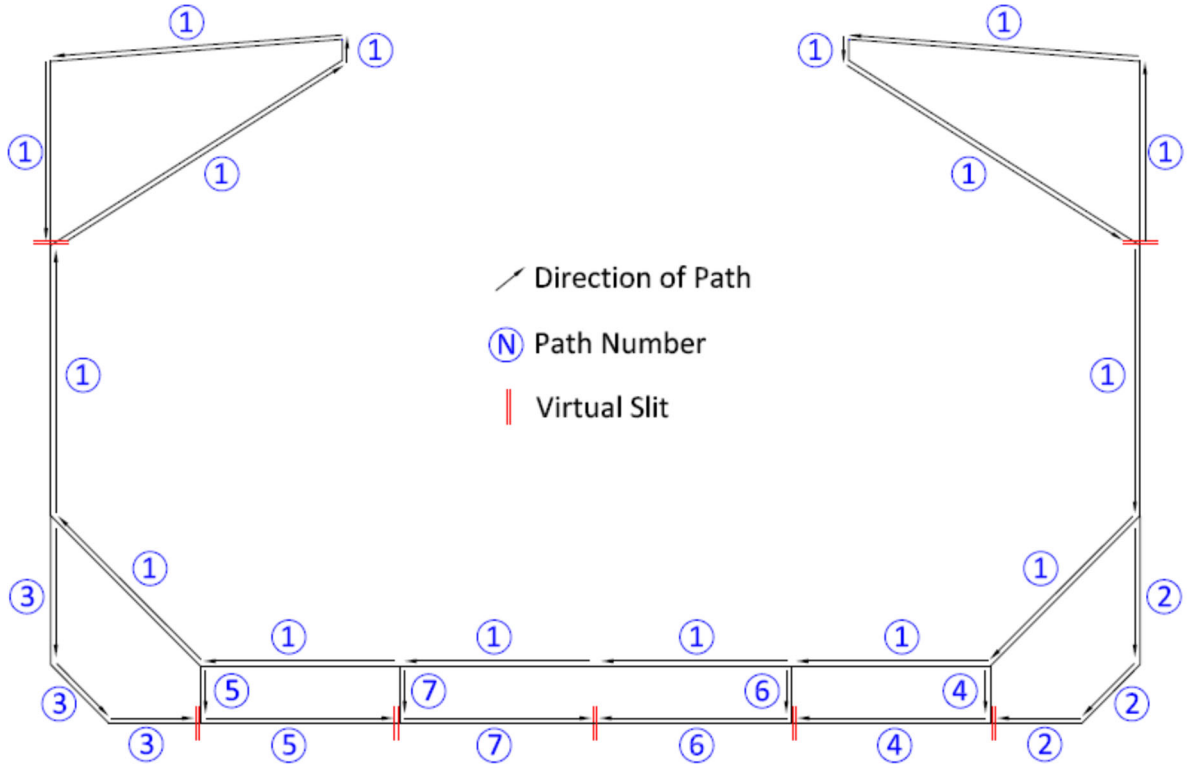

Fig. A1.2. Positions of virtual slits and paths chosen for finding sectorial coordinate (ω_{nsc})

Table A1.2: Member definition and thicknesses

Member no.	Node 1	Node 2	Thickness (m)	Member no.	Node 1	Node 2	Thickness (m)
1	0	1	0.017	16	0	13	0.017
2	1	2	0.017	17	13	14	0.017
3	2	3	0.017	18	14	15	0.017
4	3	4	0.017	19	15	16	0.017
5	4	5	0.018	20	16	17	0.018
6	5	6	0.019	21	17	18	0.019
7	6	7	0.021	22	18	19	0.021
8	7	8	0.021	23	19	8	0.021
9	5	9	0.018	24	17	20	0.018
10	9	10	0.021	25	20	21	0.021
11	10	11	0.024	26	21	22	0.024
12	11	12	0.024	27	22	23	0.024
13	12	9	0.015	28	23	20	0.015
14	2	6	0.015	29	14	18	0.015
15	1	7	0.015	30	13	19	0.015

Table A1.3: Loops, their enclosed areas and closed line integrals

Loop No.	Members (in order)	Nodes (in order)	Twice enclosed area (clockwise -ve) (m^2)	$\oint \frac{ds}{t(s)}$
1	2-14-7-15	1-2-6-7-1	19.824	852.011
2	3-4-5-6-14	2-3-4-5-6-2	31.569	988.294
3	10-11-12-13	9-10-11-12-9	52.384	1327.484
4	17-29-22-30	13-14-18-19-13	-19.824	852.011
5	18-19-20-21-29	14-15-16-17-18-14	-31.569	988.294
6	25-26-27-28	20-21-22-23-20	-52.384	1327.484
7	1-15-8-23-30-16	0-1-7-8-19-13-0	38.976	1458.734

Table A1.3 gives the loops chosen for calculation of the indeterminate properties. Unit Saint-Venant torsion T_{SV} is applied, and using (3.6) and Table A1.3, the set of simultaneous equations (A1.1) is arrived at. On solving (A1.1), (A1.2) is obtained from which the Saint-Venant torsion constant (J) is found using (A1.3). The Saint-Venant statical moment is calculated as per (3.9) and given in Table A1.4.

$$\begin{bmatrix} 852.011 & -112.000 & 0 & 0 & 0 & 0 & -112.000 & -19.824 \\ -112.000 & 988.294 & 0 & 0 & 0 & 0 & 0 & -31.569 \\ 0 & 0 & 1327.484 & 0 & 0 & 0 & 0 & -52.384 \\ 0 & 0 & 0 & 852.011 & -112.000 & 0 & 112.000 & 19.824 \\ 0 & 0 & 0 & -112.000 & 988.294 & 0 & 0 & 31.569 \\ 0 & 0 & 0 & 0 & 0 & 1327.484 & 0 & 52.384 \\ -112.000 & 0 & 0 & 112.000 & 0 & 0 & 1458.734 & -38.976 \\ 19.824 & 31.569 & 52.384 & -19.824 & -31.569 & -52.384 & 38.976 & 0.00035 \end{bmatrix} \begin{bmatrix} q_1^{id} \\ q_2^{id} \\ q_3^{id} \\ q_4^{id} \\ q_5^{id} \\ q_6^{id} \\ q_7^{id} \\ G\emptyset' \end{bmatrix}$$

$$= \begin{bmatrix} 0 \\ 0 \\ 0 \\ 0 \\ 0 \\ 0 \\ 0 \\ 1 \end{bmatrix} \quad (A1.1)$$

$$\begin{bmatrix} q_1^{id} \\ q_2^{id} \\ q_3^{id} \\ q_4^{id} \\ q_5^{id} \\ q_6^{id} \\ q_7^{id} \\ G\emptyset' \end{bmatrix} = \begin{bmatrix} 3.612 \\ 4.003 \\ 4.440 \\ -3.612 \\ -4.003 \\ -4.440 \\ 3.561 \\ 112.517 \end{bmatrix} \times 10^{-3} \quad (A1.2)$$

$$J = \frac{1}{G\emptyset'} = \frac{1}{0.112517} = 8.888\ m^4 \quad (A1.3)$$

Table A1.4: Indeterminate S_{SV} within loops

Cell. No. (j)	Loop direction	$S_{SV,j}^{id} = q_j^{id} \times J/1$ m^2
1	Anti-clockwise	-0.0321
2	Anti-clockwise	-0.0356
3	Anti-clockwise	-0.0395
4	Clockwise	0.0321
5	Clockwise	0.0356
6	Clockwise	0.0395
7	Anti-clockwise	-0.0316

The set of paths chosen is as given in the first four columns (A-D) of Table A1.5. The temporary determinate ω_c^d is calculated as per (3.1) about the centroid as the pole, as given in columns E and F. As indicated in section 3, S_{SV} is zero in open parts of the section, and piecewise constant between two consecutive nodes, i.e., constant in a given member. S_{SV}'s given in Table A1.4 are then superimposed to find the distribution of S_{SV} in the section. Hence, the distribution of S_{SV} is given in a column G as a single column. The second term of right hand side of (3.10) is given in columns H and I. As per (3.10),

ω_c is obtained by adding columns 8 and 9 to 5 and 6, and given in columns J and K, respectively. Normalization is carried out as given in column L, and this gives ω_{nc} as shown in columns M and N. $I_{y\omega}$ and $I_{z\omega}$ are then calculated and given in columns O and P. The shear center coordinates are then found by (A1.4). Some steps are illustrated below.

The starting node for integration ($s = 0$) is chosen as node number 9. Hence, ω_{0c} is zero at that node in the first step. Member 10 is chosen as the first member in the first path, and the direction of traverse is node 9 to node 10. Hence, for a straight member, we have as per (3.1):

$$\overrightarrow{\boldsymbol{\omega_{0c}}}(node\ 10) = \overrightarrow{\boldsymbol{\omega_{0c}}}(node\ 9) + \int_0^s \left(\vec{\boldsymbol{r}}(s) - \vec{\boldsymbol{r}_c}(s)\right) \times \overrightarrow{\boldsymbol{ds}}$$

$$= \overrightarrow{\boldsymbol{\omega_{0c}}}(node\ 9) + \left(\vec{\boldsymbol{r}}(s) - \vec{\boldsymbol{r}_c}(s)\right) \times \overrightarrow{\Delta \boldsymbol{s}}$$

$$= \omega_{0c}(node\ 9) + (y_9 - y_c)(z_{10} - z_c) - (y_{10} - y_c)(z_9 - z_c)$$

$$= 0.0 + (16.13 - 0)(19.6 - 8.255) - (16.13 - 0)(14.15 - 8.255)$$

$$= 87.9085\ m^2$$

The next path starts at node 5 which has previously been visited in path 1. The value of ω_{0c} for node 5 in path 2 is same as its value encountered in path 1, i.e., -77.3 m^2. The term Ω_{SV} is calculated in a similar manner using column G, except that the formula is different. For a straight member of uniform thickness, following is the calculation:

$$\boldsymbol{\Omega_{SV}}(node\ 10) = \boldsymbol{\Omega_{SV}}(node\ 9) + \int_0^s \frac{S_{SV}(s)}{t(s)} ds$$

$$= \boldsymbol{\Omega_{SV}}(node\ 9) + \frac{S_{SV}(member\ 10)}{t(member\ 10)} Length(member\ 10)$$

$$= -10.2\ m^2$$

Table A1.5: Finding ω_{nc}, $I_{y\omega}$ and $I_{z\omega}$ for the purpose of finding shear center coordinates

A	B	C	D	E	F	G	H	I	J	K	L	M	N	O	P
Path No	Member	Node 1	Node 2	$\boldsymbol{\omega_{0c}} = \int_{s_1}^{s_2}(\vec{r} - \vec{r_c}) \times \vec{ds}$		$\boldsymbol{S_{SV}}$ after superposition	$\boldsymbol{\Omega_{SV}} = \int_{s_1}^{s_2} \frac{S_{SV}(s)}{t(s)} ds$		$\boldsymbol{\omega_c} = \omega_{0c} + \Omega_{SV}$		$\int_{s_1}^{s_2} \omega_c\, ds$	$\boldsymbol{\omega_{nc}} = \omega_c - \omega_{c,avg}$		$\boldsymbol{I_{y\omega}} = \int_{s_1}^{s_2} \omega_{nc}\, z dA$	$\boldsymbol{I_{z\omega}} = \int_{s_1}^{s_2} \omega_{nc}\, y dA$
				m^2	m^2	m^2	m^2	m^2	m^2	m^2	m^2	m^2	m^2	m^5	m^5
1	10	9	10	0.0	87.9	-0.0395	0.0	-10.2	0.0	77.7	211.6	317.1	394.7	355.1	657.0
	11	10	11	87.9	196.3	-0.0395	-10.2	-24.5	77.7	171.8	1079.6	394.7	488.9	1072.0	1070.2
	12	11	12	196.3	191.6	-0.0395	-24.5	-25.5	171.8	166.2	104.8	488.9	483.2	84.5	54.2
	13	12	9	191.6	52.4	-0.0395	-25.5	-52.4	166.2	0.0	849.3	483.2	317.1	541.5	706.6
	9	9	5	52.4	-77.3	0.0000	-52.4	-52.4	0.0	-129.7	-521.3	317.1	187.4	81.0	588.8
	6	5	6	-77.3	-158.3	-0.0356	-52.4	-64.1	-129.7	-222.4	-1102.8	187.4	94.7	-69.1	237.7
	7	6	7	-158.3	-197.1	-0.0321	-64.1	-73.1	-222.4	-270.2	-1453.1	94.7	46.9	-57.7	79.7

	8	7	8	-197.1	-235.2	-0.0316	-73.1	-81.9	-270.2	-317.1	-1703.0	46.9	0.0	-18.8	11.0
	23	8	19	-235.2	-273.3	-0.0316	-81.9	-90.6	-317.1	-363.9	-1974.9	0.0	-46.9	18.8	11.0
	22	19	18	-273.3	-312.1	-0.0321	-90.6	-99.6	-363.9	-411.8	-2288.3	-46.9	-94.7	57.7	79.7
	21	18	17	-312.1	-393.1	-0.0356	-99.6	-111.4	-411.8	-504.4	-2870.0	-94.7	-187.4	69.1	237.7
	24	17	20	-393.1	-522.8	0.0000	-111.4	-111.4	-504.4	-634.1	-4577.1	-187.4	-317.1	-81.0	588.8
	28	20	23	-522.8	-662.0	-0.0395	-111.4	-138.3	-634.1	-800.3	-7332.0	-317.1	-483.2	-541.5	706.6
	27	23	22	-662.0	-666.7	-0.0395	-138.3	-139.3	-800.3	-806.0	-497.9	-483.2	-488.9	-84.5	54.2
	26	22	21	-666.7	-558.3	-0.0395	-139.3	-153.5	-806.0	-711.8	-6567.7	-488.9	-394.7	-1072.0	1070.2
	25	21	20	-558.3	-470.4	-0.0395	-153.5	-163.8	-711.8	-634.1	-3667.7	-394.7	-317.1	-355.1	657.0
2	5	5	4	-77.3	-148.1	0.0356	-52.4	-43.7	-129.7	-191.8	-705.7	187.4	125.2	-51.8	199.2
	4	4	3	-148.1	-187.0	0.0356	-43.7	-38.6	-191.8	-225.7	-506.3	125.2	91.4	-32.8	68.4
	3	3	2	-187.0	-209.5	0.0356	-38.6	-32.9	-225.7	-242.4	-636.6	91.4	74.6	-31.7	50.3
3	20	17	16	-393.1	-322.3	-0.0356	-111.4	-120.0	-504.4	-442.3	-2078.1	-187.4	-125.2	51.8	199.2
	19	16	15	-322.3	-283.3	-0.0356	-120.0	-125.1	-442.3	-408.5	-1031.7	-125.2	-91.4	32.8	68.4
	18	15	14	-283.3	-260.9	-0.0356	-125.1	-130.8	-408.5	-391.7	-1088.2	-91.4	-74.6	31.7	50.3
4	14	6	2	-158.3	177.9	-0.0035	-64.1	-64.5	-222.4	-242.4	-390.4	94.7	74.6	-15.8	25.0
	2	2	1	-177.9	-226.6	0.0321	-64.5	-53.4	-242.4	-280.0	-1541.1	74.6	37.1	-46.3	50.9
5	29	18	14	-312.1	292.5	0.0035	-99.6	-99.2	-411.8	-391.7	-674.9	-94.7	-74.6	15.8	25.0
	17	14	13	-292.5	-243.8	-0.0321	-99.2	-110.4	-391.7	-354.1	-2200.3	-74.6	-37.1	46.3	50.9
6	15	7	1	-197.1	206.8	-0.0005	-73.1	-73.2	-270.2	-280.0	-462.1	46.9	37.1	-7.8	6.1
	1	1	0	-206.8	-254.7	0.0316	-73.2	-62.4	-280.0	-317.1	-1731.4	37.1	0.0	-15.1	7.1
7	30	19	13	-273.3	263.6	0.0005	-90.6	-90.6	-363.9	-354.1	-603.2	-46.9	-37.1	7.8	6.1
	16	13	0	-263.6	-215.7	-0.0316	-90.6	-101.4	-354.1	-317.1	-1946.5	-37.1	0.0	15.1	7.1
							$\int_\Omega \omega_c\, ds$				-47907.2			0.000	7624.5
							$\omega_{c,avg} = \frac{1}{\int_\Omega ds}\left(\int_\Omega \omega_{cg}\, ds\right)$				-317.066			$I_{y\omega}$	$I_{z\omega}$

$$y_{sc,o} = y_{cg,o} + \frac{I_{zz}I_{y\omega} - I_{yz}I_{z\omega}}{I_{yy}I_{zz} - I_{yz}I_{yz}} = 0.000\ m$$
$$z_{sc,o} = z_{cg,o} + \frac{I_{yz}I_{y\omega} - I_{yy}I_{z\omega}}{I_{yy}I_{zz} - I_{yz}I_{yz}} = 8.255 - \frac{1352089}{73360} = -10.176\ m \qquad (A1.4)$$

Once the shear center is found, the entire procedure of Table A1.5 is repeated till normalization (column N), this time with the shear center as the pole instead of the centroid, as given in Table A1.6 till column

N. This gives ω_{nsc} using which the warping constant $I_{\omega\omega}$ is calculated as given in column O. The principal sectorial coordinate is then compiled and given in Table A1.7.

Table A1.6: Finding the principal sectorial coordinate.

A	B	C	D	E	F	G	H	I	J	K	L	M	N	O
Path No	Member	Node 1	Node 2	$\omega_{0sc} = \int_{s_1}^{s_2}(\vec{r} - \overrightarrow{r_{sc}}) \times d\vec{s}$		S_{sv} after superpositio	$\Omega_{sv} = \int_{s_1}^{s_2} \frac{S_{sv}(s)}{t(s)} ds$		$\omega_{sc} = \omega_{0sc} + \Omega_{sv}$		$\int_{s_1}^{s_2} \omega_{sc}\, ds$	$\omega_{nsc} = \omega_{sc} - \omega_{sc,avg}$		$I_{\omega\omega} = \int_{s_1}^{s_2} \omega_{nsc}^2 dA$
				m²	m²	m²	m²	m²	m²	m²	m²	m²	m²	m⁶
1	10	9	10	0.00	87.91	-0.0395	0.0	-10.2	0.00	77.67	211.64	19.78	97.44	450.70
	11	10	11	87.91	355.36	-0.0395	-10.2	-24.5	77.67	330.89	1767.90	97.44	350.66	11536.78
	12	11	12	355.36	350.71	-0.0395	-24.5	-25.5	330.89	325.22	203.39	350.66	344.99	1800.30
	13	12	9	350.71	52.38	-0.0395	-25.5	-52.4	325.22	0.00	1662.33	344.99	19.78	6452.44
	9	9	5	52.38	-77.30	0.0000	-52.4	-52.4	0.00	-129.69	-521.33	19.78	-109.91	496.74
	6	5	6	-77.30	-76.61	-0.0356	-52.4	-64.1	-129.69	-140.73	-847.06	-109.91	-120.95	1587.21
	7	6	7	-76.61	-6.66	-0.0321	-64.1	-73.1	-140.73	-79.80	-650.55	-120.95	-60.02	1052.79
	8	7	8	-6.66	62.10	-0.0316	-73.1	-81.9	-79.80	-19.78	-288.77	-60.02	0.00	146.27
	23	8	19	62.10	130.86	-0.0316	-81.9	-90.6	-19.78	40.24	59.35	0.00	60.02	146.27
	22	19	18	130.86	200.81	-0.0321	-90.6	-99.6	40.24	101.17	417.18	60.02	120.95	1052.79
	21	18	17	200.81	201.50	-0.0356	-99.6	-111.4	101.17	90.13	599.25	120.95	109.91	1587.21
	24	17	20	201.50	71.82	0.0000	-111.4	-111.4	90.13	-39.55	203.31	109.91	-19.78	496.74
	28	20	23	71.82	-226.51	-0.0395	-111.4	-138.3	-39.55	-364.77	-2066.69	-19.78	-344.99	6452.44
	27	23	22	-226.51	-231.16	-0.0395	-138.3	-139.3	-364.77	-370.44	-227.92	-344.99	-350.66	1800.30
	26	22	21	-231.16	36.29	-0.0395	-139.3	-153.5	-370.44	-117.22	-2110.23	-350.66	-97.44	11536.78
	25	21	20	36.29	124.20	-0.0395	-153.5	-163.8	-117.22	-39.55	-427.22	-97.44	-19.78	450.70
2	5	5	4	-77.30	-148.11	0.0356	-52.4	-43.7	-129.69	-191.82	-705.70	-109.91	-172.04	1595.84
	4	4	3	-148.11	-155.51	0.0356	-43.7	-38.6	-191.82	-194.14	-468.05	-172.04	-174.37	1236.94
	3	3	2	-155.51	-127.84	0.0356	-38.6	-32.9	-194.14	-160.77	-482.69	-174.37	-141.00	1153.97
3	20	17	16	201.50	272.31	-0.0356	-111.4	-120.0	90.13	152.26	532.05	109.91	172.04	1595.84
	19	16	15	272.31	279.71	-0.0356	-120.0	-125.1	152.26	154.59	372.12	172.04	174.37	1236.94
	18	15	14	279.71	252.04	-0.0356	-125.1	-130.8	154.59	121.22	375.10	174.37	141.00	1153.97
4	14	6	2	-76.61	-96.27	-0.0035	-64.1	-64.5	-140.73	-160.77	-253.26	-120.95	-141.00	433.12
	2	2	1	-96.27	-36.23	0.0321	-64.5	-53.4	-160.77	-89.59	-738.58	-141.00	-69.82	1156.73

5	29	18	14	200.81	220.47	0.0035	-99.6	-99.2	101.17	121.22	186.81	120.95	141.00	433.12
	17	14	13	220.47	160.43	-0.0321	-99.2	-110.4	121.22	50.04	505.21	141.00	69.82	1156.73
6	15	7	1	-6.66	-16.41	-0.0005	-73.1	-73.2	-79.80	-89.59	-142.29	-60.02	-69.82	106.41
	1	1	0	-16.41	42.61	0.0316	-73.2	-62.4	-89.59	-19.78	-317.18	-69.82	0.00	160.20
7	30	19	13	130.86	140.61	0.0005	-90.6	-90.6	40.24	50.04	75.84	60.02	69.82	106.41
	16	13	0	140.61	81.59	-0.0316	-90.6	-101.4	50.04	-19.78	87.76	69.82	0.00	160.20
							$\int_\Omega \omega_{sc}\, ds$				-2988.3			58732.86
							$\omega_{sc,avg} = \frac{1}{\int_\Omega ds}\left(\int_\Omega \omega_{cg}\, ds\right)$				-19.778			$I_{\omega\omega}$

Table A1.7: Compiled node-wise sectorial coordinates obtained by manual calculations

Node no.	*y* (m)	*z* (m)	ω_{nsc} (m^2)	Node no.	*y* (m)	*z* (m)	ω_{nsc} (m^2)
0	0.00	0.00	0.00	12	7.50	19.63	344.99
1	5.80	0.00	-69.82	13	-5.80	0.00	69.82
2	11.70	0.00	-141.00	14	-11.70	0.00	141.00
3	14.42	0.00	-174.37	15	-14.42	0.00	174.37
4	16.13	1.72	-172.04	16	-16.13	1.72	172.04
5	16.13	6.11	-109.91	17	-16.13	6.11	109.91
6	11.70	1.68	-120.95	18	-11.70	1.68	120.95
7	5.80	1.68	-60.02	19	-5.80	1.68	60.02
8	0.00	1.68	0.00	20	-16.13	14.15	-19.78
9	16.13	14.15	19.78	21	-16.13	19.60	-97.44
10	16.13	19.60	97.44	22	-7.50	20.25	-350.66
11	7.50	20.25	350.66	23	-7.50	19.63	-344.99

Table A1.8: Comparison of section properties between ANSYS & manual calculations

Sl. No.	Item	Symbol	Component	Units	Values / Results	
					Manual	ANSYS
1	Position of Centroid	y_{cg}	Y	m	0.000	0.000
		z_{cg}	Z	m	8.255	8.258
2	Position of Shear Center	y_{sc}	Y	m	0.000	0.000
		z_{sc}	Z	m	-10.176	-10.180
3	Area of the section	*A*	-	m^2	2.831	2.829
3	Moment of Inertia	I_{yy}	YY	m^4	177.335	177.259
		I_{zz}	ZZ	m^4	413.681	413.367
		I_{yz}	YZ	m^4	0.000	0.000
4	Saint-Venant Constant	*J*	-	m^4	8.888	8.908
5	Warping Constant	$I_{\omega\omega}$	-	m^6	58732.865	58718.216

Table A1.8 lists the overall section properties evaluated using the above procedure. Once the sectorial coordinate and the warping constant are found, the next step is to calculate the statical moments and the sectorial statical moment. For this, a new set of paths has to be chosen. Fig. A1.3 shows the paths and position of virtual slits used for manual calculations at this stage.

The calculation of the determinate part of the statical moments and the sectorial statical moment is given in Table A1.9. The first four columns (A - D) give the set of paths chosen. Column E and F give

the values of the normalized principal sectorial coordinate ω_{nsc} corresponding to the nodes in column C and D. The determinate part of $S_{\omega s}$ is then calculated using (3.3) and given in column G and H. The indeterminate part of $S_{\omega s}$ is then calculated using the determinate part of $S_{\omega s}$ from Table A1.9. The calculations have been shown in Table A1.10. The coefficients given in (A1.5) are extracted from Table A1.10. These coefficients have been given a dark-grey shade in Table A1.10. On solving the set of simultaneous equations (A1.5), the indeterminate part of $S_{\omega s}$ are found as given in Table A1.11. The determinate and the indeterminate shear flows from Table A1.9 and Table A1.11 respectively are then superimposed taking into account the directions of the loops and paths (addition if direction the direction of loop and member is same, subtraction otherwise), and the final values of $S_{\omega s}$ are obtained as given in Table A1.12.

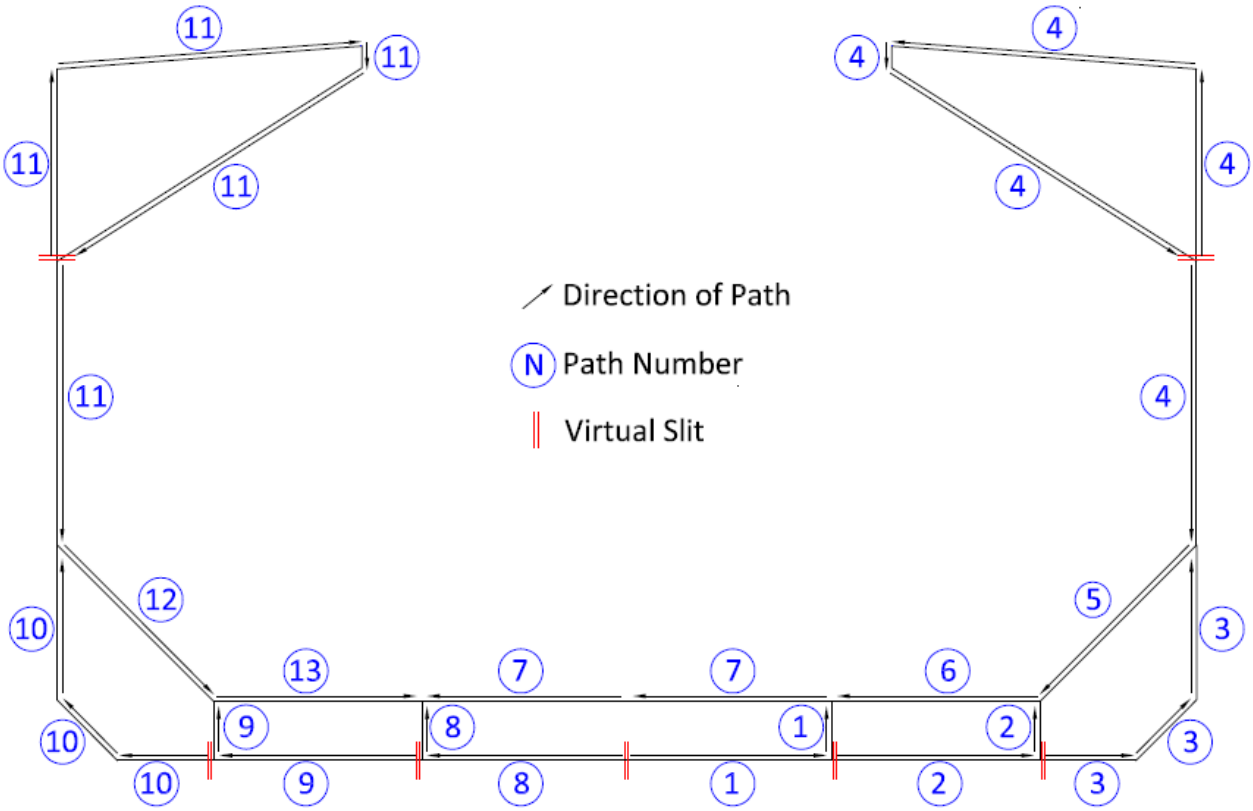

Fig. A1.3. Chosen virtual slits and paths for finding the sectorial statical moment ($S_{\omega s}$)

An example is illustrated as to how (A1.5) (or similarly, (A1.1)) is arrived at. Loop 4 has members 29 and 30 common with loops 5 and 7, respectively. The direction of integration between loops 4 and 5 along member 29 is in the opposite, and that between loops 4 and 7 along member 30 is in the same sense. Hence, for the term in position (4, 5) in (3.6), χ_{12} is -1 for member 29 and zero for the rest of the members, as per (3.7). Similarly for the term in position (4, 7) in (3.6), χ_{12} is 1 for member 30 and zero for the rest of the members of loop 4 as per (3.7). Hence, the final values at positions (4, 5) and (4, 7) in (A1.1) as well as (A1.5) are -112.000 and 112.000, respectively.

Table A1.9: Finding the determinate part of $S_{\omega s}$

	A	B	C	D	E	F	G	H	I
1	Path No	Member	Node 1	Node 2	ω_{nsc} Node 1	ω_{nsc} Node 2	$S^d_{\omega s}$		Remarks
							$S^d_{\omega s}(s_1)$	$S^d_{\omega s}(s_2)$	
							$\Delta S^d_{\omega s} \overset{\text{def}}{\equiv} \int_{s_1}^{s_2} \omega_{nsc} dA$		
							m^4	m^4	
2	1	1	0	1	0.00	-69.82	0.000	-3.442	Virtual slit
3		15	1	7	-69.82	-60.02	-3.442	-5.078	
4	2	2	1	2	-69.82	-141.00	0.000	-10.572	Virtual slit
5		14	2	6	-141.00	-120.95	-10.572	-13.873	
6	3	3	2	3	-141.00	-174.37	0.000	-7.291	Virtual slit
7		4	3	4	-174.37	-172.04	-7.291	-14.433	
8		5	4	5	-172.04	-109.91	-14.433	-25.572	
9	4	10	9	10	19.78	97.44	0.000	6.708	Virtual slit
10		11	10	11	97.44	350.66	6.708	53.246	
11		12	11	12	350.66	344.99	53.246	58.421	
12		13	12	9	344.99	19.78	58.421	86.389	
13		9	9	5	19.78	-109.91	86.389	79.867	
14	5	6	5	6	-109.91	-120.95	54.295	40.555	G14 = H8 + H13
15	6	7	6	7	-120.95	-60.02	26.682	15.471	G15 = H5 + H14
16	7	8	7	8	-60.02	0.00	10.393	6.737	G16 = H3 + H15
17		23	8	19	0.00	60.02	6.737	10.393	
18	8	16	0	13	0.00	69.82	0.000	3.442	Virtual slit
19		30	13	19	69.82	60.02	3.442	5.078	
20	9	17	13	14	69.82	141.00	0.000	10.572	Virtual slit
21		29	14	18	141.00	120.95	10.572	13.873	
22	10	18	14	15	141.00	174.37	0.000	7.291	Virtual slit
23		19	15	16	174.37	172.04	7.291	14.433	
24		20	16	17	172.04	109.91	14.433	25.572	
25	11	25	20	21	-19.78	-97.44	0.000	-6.708	Virtual slit
26		26	21	22	-97.44	-350.66	-6.708	-53.246	
27		27	22	23	-350.66	-344.99	-53.246	-58.421	
28		28	23	20	-344.99	-19.78	-58.421	-86.389	
29		24	20	17	-19.78	109.91	-86.389	-79.867	
30	12	21	17	18	109.91	120.95	-54.295	-40.555	G30 = H24 + H29
31	13	22	18	19	120.95	60.02	-26.682	-15.471	G31 = H21 + H30

$$\begin{bmatrix} 852.011 & -112.000 & 0 & 0 & 0 & 0 & -112.000 \\ -112.000 & 988.294 & 0 & 0 & 0 & 0 & 0 \\ 0 & 0 & 1327.484 & 0 & 0 & 0 & 0 \\ 0 & 0 & 0 & 852.011 & -112.000 & 0 & 112.000 \\ 0 & 0 & 0 & -112.000 & 988.294 & 0 & 0 \\ 0 & 0 & 0 & 0 & 0 & 1327.484 & 0 \\ -112.000 & 0 & 0 & 112.000 & 0 & 0 & 1458.734 \end{bmatrix} \begin{bmatrix} S^{id}_{\omega,1} \\ S^{id}_{\omega,2} \\ S^{id}_{\omega,3} \\ S^{id}_{\omega,4} \\ S^{id}_{\omega,5} \\ S^{id}_{\omega,6} \\ S^{id}_{\omega,7} \end{bmatrix}$$

$$= \begin{bmatrix} -3222.362 \\ -9955.637 \\ -63528.178 \\ 3222.362 \\ 9955.637 \\ 63528.178 \\ -2652.961 \end{bmatrix} (A1.5)$$

Table A1.10: Finding indeterminate part of $S_{\omega s}$

Loop	Mem -ber	Node 1	Node 2	$S_{\omega s}$	$\oint \frac{ds}{t(s)}$	ϕ_ω	Remarks
LOOP 1							
1	2	1	2	0.00	347.06	-1628.12	
	14	2	6	-10.57	112.00	-1373.64	Common edge with loop 2
	7	6	7	26.68	280.95	5744.70	
	15	7	1	5.08	112.00	479.42	Common edge with loop 7
					852.01	**3222.36**	Total
LOOP 2							
2	3	2	3	0.00	160.00	-562.72	
	4	3	4	-7.29	142.67	-1550.80	
	5	4	5	-14.43	243.89	-4978.18	
	6	5	6	54.29	329.74	15673.70	
	14	6	2	13.87	112.00	1373.64	Common edge with loop 1
					988.29	**9955.64**	Total
LOOP 3							
3	10	9	10	0.00	259.52	678.21	
	11	10	11	6.71	360.60	9229.20	
	12	11	12	53.25	25.83	1442.55	
	13	12	9	58.42	681.53	52178.22	
					1327.48	**63528.18**	Total
LOOP 4							
4	17	13	14	0.00	347.06	1628.12	
	29	14	18	10.57	112.00	1373.64	Common edge with loop 5
	22	18	19	-26.68	280.95	-5744.70	
	30	19	13	-5.08	112.00	-479.42	Common edge with loop 7
					852.01	**-3222.36**	Total
LOOP 5							
5	18	14	15	0.00	160.00	562.72	
	19	15	16	7.29	142.67	1550.80	
	20	16	17	14.43	243.89	4978.18	
	21	17	18	-54.29	329.74	-15673.70	
	29	18	14	-13.87	112.00	-1373.64	Common edge with loop 4
					988.29	**-9955.64**	Total
LOOP 6							
6	25	20	21	0.00	259.52	-678.21	
	26	21	22	-6.71	360.60	-9229.20	
	27	22	23	-53.25	25.83	-1442.55	
	28	23	20	-58.42	681.53	-52178.22	
					1327.48	**-63528.18**	Total
LOOP 7							
7	1	0	1	0.00	341.18	-391.44	
	15	1	7	-3.44	112.00	-479.42	Common edge with loop 1
	8	7	8	10.39	276.19	2197.34	
	23	8	19	6.74	276.19	2197.34	
	30	19	13	-5.08	112.00	-479.42	Common edge with loop 4
	16	13	0	-3.44	341.18	-391.44	
					1458.73	**2652.96**	Total

Table A1.11: Indeterminate $S_{\omega s}$ within loops on solving (A1.5)

Cell. No. (j)	Loop direction	$S^{id}_{\omega,j}$ m^4
1	Anti-clockwise	-5.540
2	Anti-clockwise	-10.701
3	Anti-clockwise	-47.856
4	Clockwise	5.540
5	Clockwise	10.701
6	Clockwise	47.856
7	Anti-clockwise	-2.669

Table A1.12: Final values of $S_{\omega s}$ obtained from calculations

1	2	3	4	9	10
Path No	Member	Node 1	Node 2	$S_{\omega s}$	
				$S_{\omega s}(s_1)$ m^4	$S_{\omega s}(s_2)$ m^4
1	1	0	1	-2.67	-6.11
	15	1	7	-0.57	-2.21
2	2	1	2	-5.54	-16.11
	14	2	6	-5.41	-8.71
3	3	2	3	-10.70	-17.99
	4	3	4	-17.99	-25.13
	5	4	5	-25.13	-36.27
4	10	9	10	-47.86	-41.15
	11	10	11	-41.15	5.39
	12	11	12	5.39	10.57
	13	12	9	10.57	38.53
	9	9	5	86.39	79.87
5	6	5	6	43.59	29.85
6	7	6	7	21.14	9.93
7	8	7	8	7.72	4.07
	23	8	19	4.07	7.72
8	16	0	13	2.67	6.11
	30	13	19	0.57	2.21
9	17	13	14	5.54	16.11
	29	14	18	5.41	8.71
10	18	14	15	10.70	17.99
	19	15	16	17.99	25.13
	20	16	17	25.13	36.27
11	25	20	21	47.86	41.15
	26	21	22	41.15	-5.39
	27	22	23	-5.39	-10.57
	28	23	20	-10.57	-38.53
	24	20	17	-86.39	-79.87
12	21	17	18	-43.59	-29.85
13	22	18	19	-21.14	-9.93

Appendix 2 - Illustration evaluation of response of Container Ship Hull Girder to Torsion Loads

The principal particulars of a container ship hull girder midship section including its stiffeners are given below:

Length Overall (L_{OA})	299.00 m
Length between Perpendiculars (L)	285.20 m
Length Scantling (L_S)	282.60 m
Breadth (Moulded) (B)	40.00 m
Depth (H)	24.40 m
Design Draft (Moulded) (T_d)	12.00 m
Scantling Draft (Moulded) (T)	14.50 m
Block Coefficient (C_B)	0.669

The cross-section properties of the midship section are given in Table A2.1, and the cross-section is shown in Fig. A2.1. The origin of the global coordinate system is at the intersection of the centerline with the baseline.

Table 1: Cross-section properties of the midship hull girder section

Sl. No.	Item	Symbol	Component	Units	Value
1	Position of Centroid	y_{cg}	Y	m	-0.0000
		z_{cg}	Z	m	11.0122
2	Position of Shear Center	y_{sc}	Y	m	-0.0001
		z_{sc}	Z	m	-12.6357
3	Area of the section	A	-	m^2	5.1847
3	Moment of Inertia	I_{yy}	YY	m^4	508.3210
		I_{zz}	ZZ	m^4	1366.4367
		I_{yz}	YZ	m^4	0.0025
4	Saint-Venant Constant	J	-	m^4	13.0209
5	Warping Constant	$I_{\omega\omega}$	-	m^6	120700.8254

For the purpose of illustration, the cross-sectional properties of the midship section of the ship have used along the entire length for finding the response of the ship. (In actual case the distribution of the cross-section properties along the ship length should be used.)

The torsion distribution applied along the length of the ship between perpendiculars is shown in Fig. A2.2. Note that the units of the torsion distribution in (4.1) are in Nm/m, whereas the units shown in the distribution are in Nm obtained on integration. The derivative of the distribution shown in Fig. A2.2 is the applied distribution $m_T(x)$ in (4.1).

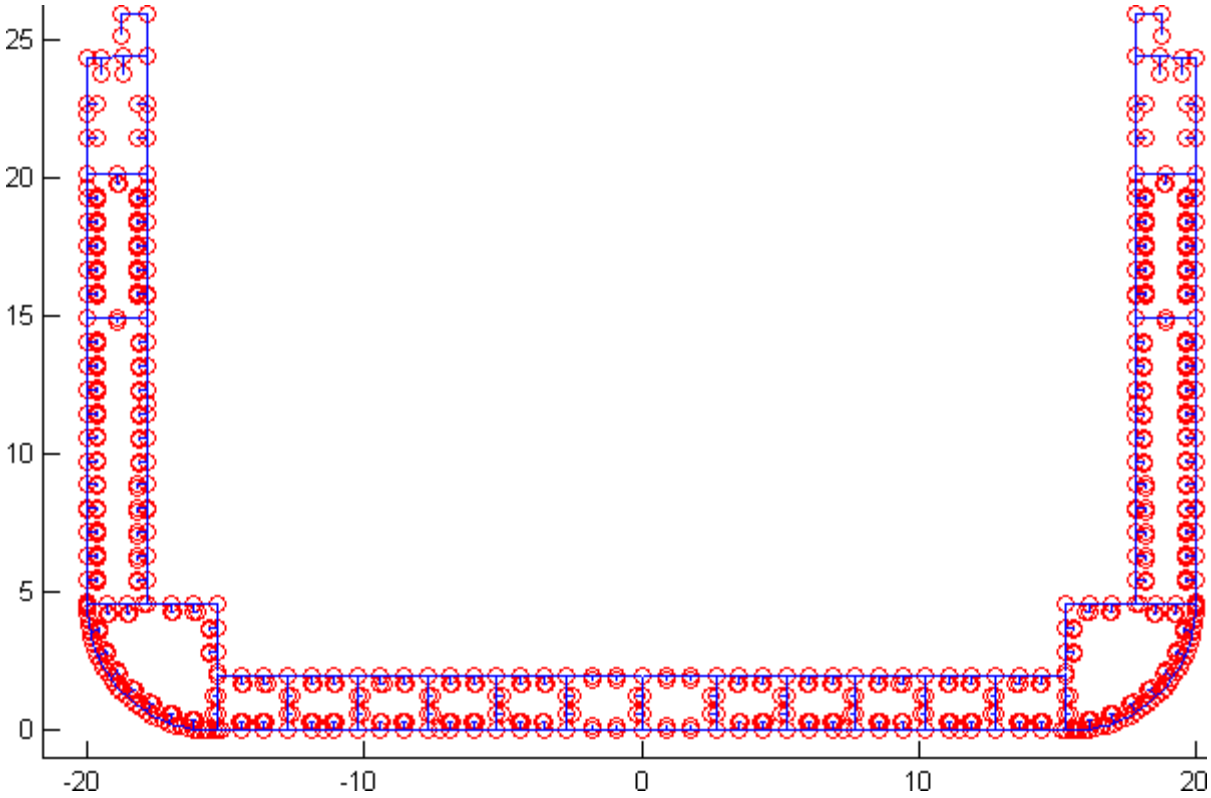

Fig. A2.1 Midship section of the chosen container ship (axes markings are in 'm')

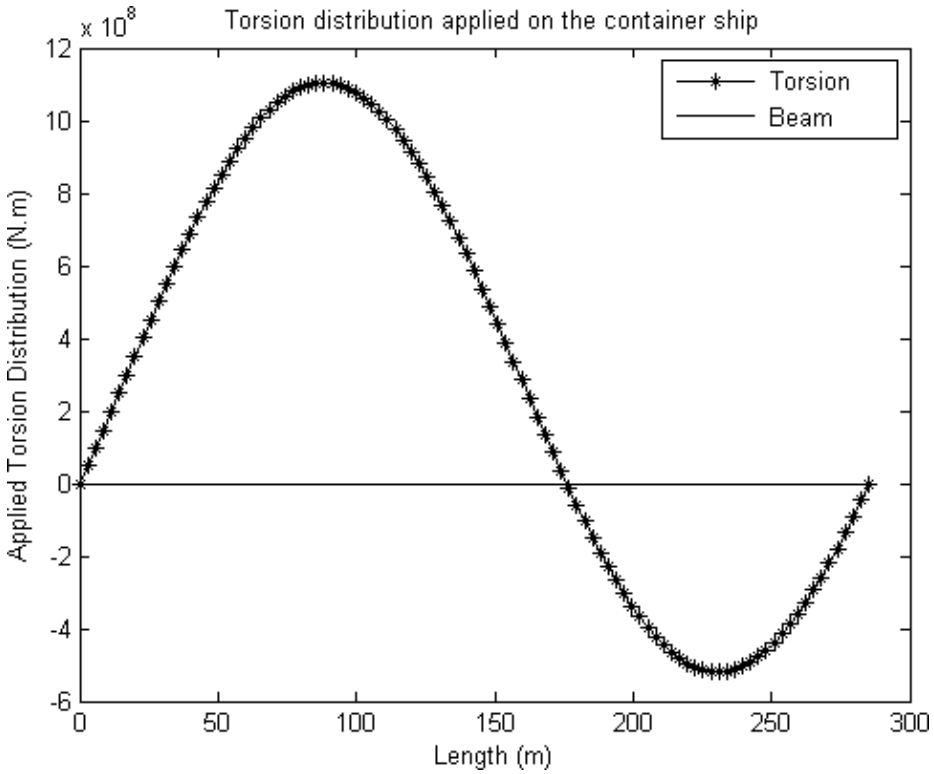

Fig. A2.2 Integrated torsion distribution (N.m) applied on the ship

Either numerical solution or finite element solution of (4.1) may be used to find the distributions of bimoment and Saint-Venant, warping and total torsions. The bimoment, Saint-Venant torsion, warping torsion and total torsion distributions generated along the length of the ship have been shown in Fig. A2.3.

The boundary conditions considered are as follows:

1. Angle of rotation fixed at engine room,
2. Warping fixed at engine room,
3. Bimoment zero at the free ends of the ship, and
4. Total torsion zero at the free ends of the ship.

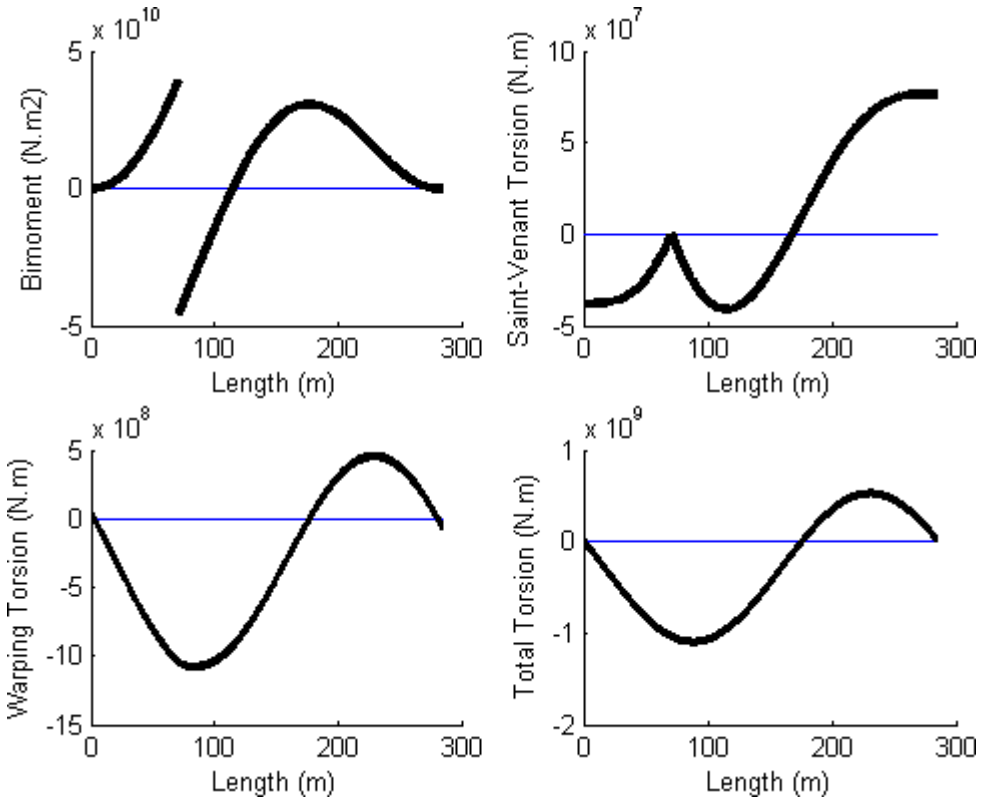

Fig. A2.3. Response of the container ship to the applied torsion distribution

The maximum value of the bimoment occurs at the forward bulkhead of the engine room, equaling 45.9 GNm^2. The maximum value of the sectorial coordinate ω is found to be 253.15 m^2 for this particular container ship lying at coordinates (17.88, 26), i.e., inner side of the hatch coaming top. Hence the maximum warping axial stress due to the maximum bimoment is:

$$\sigma_{max} = 96.241[N/mm^2] \qquad (A2.1)$$

The maximum value of the $S_{\omega s}/t_i$ for the containership is found to be 6173.4 m^4/m for this particular container ship at coordinates (17.88, 14.96), i.e., at the central portion of the inner side shell, just above a stringer. The maximum warping torsion occurs in this case occurs forward to the engine room,

equaling 1.08GNm (where the Saint-Venant torsion is zero in this case). The maximum warping shear stress due to the warping torsion is:

$$\boldsymbol{\tau_{\omega s,max} = 55.200[N/mm^2]} \qquad (A2.2)$$

However, it is to be noted that the maxima of Saint-Venant and warping torsions occur at different locations along the length of the ship. For the present case, the maximum Saint-Venant torsion occurs at the free end of the ship (note that the total torsion at the free end is zero but the individual Saint-Venant and warping torsions are non-zero), equaling only 71 MNm which is negligible (less than 1%) in comparison with the maximum warping torsion of 1.08 GNm forward to the engine room. The maximum Saint-Venant shear stress is:

$$\boldsymbol{\tau_{SV,max} = 17.283[N/mm^2]} \qquad (A2.3)$$

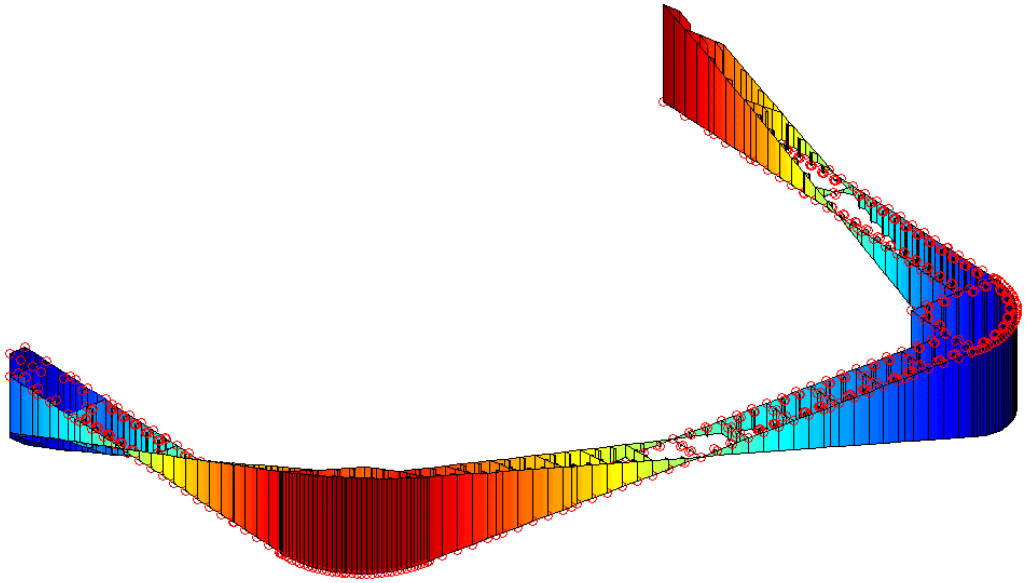

Fig. A2.4. Schematic view of axial stresses due to warping

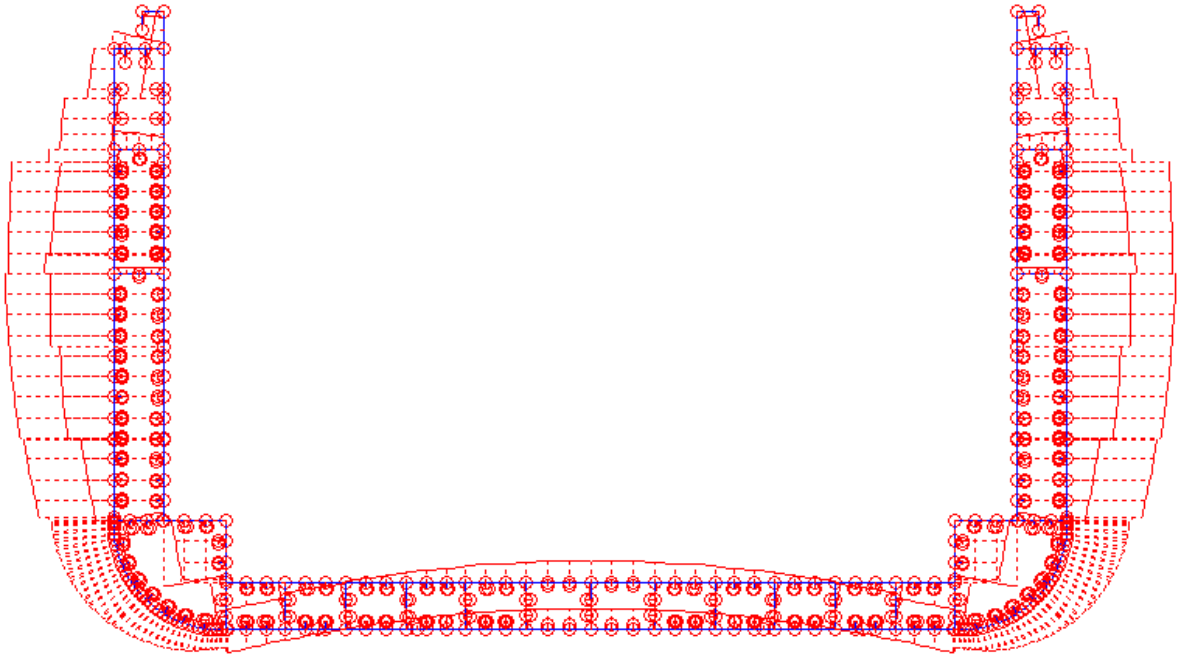

Fig. A2.5. Schematic view of distribution of the magnitude of shear stresses due to warping

End of Guidelines